Supporting Information

Achieving Giant Optical Anisotropy in the Mid-Far Infrared Wavelength via Ideal Alignment of Dual Functional Motifs

Yi-Wen Shan,[a,b] Ming-Zhi Zhang,[a,b] Chun-Li Hu,*[a] Jiang-Gao Mao*[a,b]

a: State Key Laboratory of Functional Crystals and Devices, Fujian Institute of Research on the Structure of Matter, Chinese Academy of Sciences, Fuzhou 350002 (P. R. China).

b: University of Chinese Academy of Sciences, Beijing 100049 (P. R. China).

*Corresponding authors: clhu@fjirsm.ac.cn; mjg@fjirsm.ac.cn

Section	Title	Page
S1	Experimental Section	**S3-S4**
S2	Computational Method	**S4-S5**
Table S1	Summary of crystallographic data and structure refinements for **LSSC** and **LSSB**.	**S6**
Table S2	Atomic coordinates and equivalent isotropic displacement parameters for **LSSC** and **LSSB**.	**S7**
Table S3	Selected bond distances and bond angles for **LSSC** and **LSSB**.	**S7-S8**
Table S4	Comprehensive statistics of Δn and E_g between **LSSC**, **LSSB**, and some typical chalcogenide birefringent crystals with Δn > 0.1 and E_g > 1.0 eV.	**S9-S11**
Figure S1	Comparison of Cl/Br:S molar ratios and the assembly modes of the anionic groups in **LSSB**, $La_5Sb_2S_9Cl_3$, $La_3SbS_5Cl_2$ and $LaSbS_2Br_2$.	**S12**
Figure S2	Elemental analyses of **LSSC** and **LSSB.**	**S13**
Figure S3	Simulated and experimental powder X-ray diffractometer patterns of **LSSC** and **LSSB**.	**S14**
Figure S4	The TG-DSC curves of **LSSC** and **LSSB**.	**S14**
Figure S5	The band structures of **LSSC** and **LSSB**.	**S14**
References	References	**S15-S19**

S1. Experimental Section

Reagents

The start materials are $LaCl_3$ (99.9%, Shanghai Aladdin Biochemistry Technology), $LaBr_3$ (99.9%, Shanghai Aladdin Biochemistry Technology), La_2S_3 (99.9%, Beijing Hawk Science), Sb powder (99.5%, Shanghai Aladdin Biochemistry Technology), and S powder (98%, Shanghai Aladdin Biochemistry Technology).

Syntheses

Single crystals of $La_2SbS_3(S_2)X$ (X = Cl, Br; **LSSC**, **LSSB**) were prepared via a high-temperature solid-state reaction under anhydrous and oxygen-free conditions. In an argon-filled glove box, precisely weighed $LaCl_3$/$LaBr_3$, La_2S_3, Sb, and S (molar ratio =1:2:3:8, total mass = 0.3 g) were loaded into a clean graphite crucible, and the crucible was subsequently placed into a quartz tube. The quartz tubes were flame-sealed under high vacuum (10^{-3} Pa) using a hydrogen-oxygen torch, then transferred to a computer-controlled muffle furnace. The quartz tubes were heated to 450 ℃ within 30 h and held for 12 h, then further heated to 870 ℃ at a rate of 35 ℃ h^{-1}. After maintaining the temperature for 50 h, the system was cooled to 600 ℃ in 40 h and then held there for 25 h. Finally, the tubes were cooled to 300 ℃ at a rate of 5 ℃ per hour before turning the furnace off. After the system cooled to room temperature, the obtained samples were washed by anhydrous ethanol. Orange plate-shaped single crystals (**LSSB**) and red block-shaped single crystals (**LSSC**) were obtained in a yield of about 70%, and their purity was verified by powder X-ray diffraction and energy dispersive X-ray spectroscopy analyses. These crystals exhibit good environmental stability and remain stable in air for at least several months.

Single crystal X-ray diffraction studies

Single-crystal X-ray diffraction data for **LSSC** and **LSSB** were collected on XtaLAB Synergy R, which was equipped with single source at home/near Mo X-ray sources (λ = 0.71073 Å). The CrysAlisPro software package was utilized for data reduction. For **LSSB**, numerical absorption corrections based on Gaussian integration over a multifaceted crystal model were applied. The structures of **LSSC** and **LSSB** were solved by direct methods and refined by full-matrix least-squares fitting on F^2 using SHELXL-2017 crystallographic software package.[1] All atoms were refined with anisotropic thermal parameters. The structural data were also checked

for possible missing symmetry with the program PLATON,[2] and no higher symmetry was found. The detailed crystallographic data for the two compounds were given in Table S1.

Powder X-ray diffraction studies

Powder X-ray diffraction data were collected via Rigaku MiniFlex600 diffractometer. Scanning was performed with a scan step width of 0.02° using Cu Kα radiation (λ = 1.541886 Å) at room temperature in the 2θ range of 10-70°.

Energy-dispersive X-ray spectroscopy and the elemental distribution maps

Energy-Dispersive X-ray Spectroscopy and the elemental distribution maps were carried out using a field-emission scanning electron microscope (JSM6700F) outfitted with an Oxford INCA energy-dispersive X-ray spectroscope.

Infrared spectrum

IR spectra were recorded on a Nicolet Magna 750 Fourier Transform Infrared spectrometer in the spectral range of 4000 to 400 cm^{-1}.

UV-Vis-NIR diffuse reflectance spectroscopy

The ultraviolet-visible-near-IR (UV-Vis-NIR) diffuse reflectance spectrum in the range of 200-2000 nm was collected using a PerkinElmer Lambda 950 UV-vis-NIR spectrophotometer, with a barium sulfate powder plate as a 100% reflectance reference. Absorption data were converted from the reflection data by the Kubelka-Munk function $\alpha/S = (1-R)^2/2R$ (α is the absorption coefficient, S the scattering coefficient, and R the reflectance). The band gap value is the abscissa of the intersection of the absorption edge extension line and the zero absorption.

Thermal analyses

Thermogravimetric analysis (TGA) and differential scanning calorimetry (DSC) were performed with a NETZSCH STA 449 F5 thermal analyzer, and sample powders were heated under N_2 gas atmosphere from 20 ℃ to 1000 °C at a rate of 10 °C/min.

Birefringence measurements

The birefringence measurements were carried out on a polarizing microscope (ZEISS Axio Scope. A1) equipped with a tilting compensator.

S2. Computational Method

The electronic structure and optical properties were analyzed by the plane wave pseudopotential method in the density functional theory (DFT) implemented in the total energy code CASTEP.[3,4] For the exchange and correlation functions, we chose Perdew-Burke-Ernzerhof

(PBE) in the generalized Gradient Approximation (GGA).[5] The interactions between the ionic cores and the electrons were described by the norm-conserving pseudopotential.[6] The following valence-electron configurations were considered in the computation: La $5d^16s^2$, Sb $5s^25p^3$, S $3s^23p^4$, and Cl $3s^23p^5$/Br $4s^24p^5$. The numbers of plane waves included in the basis sets were determined by cutoff energies of 750 eV (**LSSC**) and 650 eV (**LSSB**). Monkhorst-Pack k-point sampling of 3×5×1 was used to perform numerical integration of the Brillouin zone. During the optical property calculations, approximately 192 empty bands were involved to ensure the convergence of linear optical properties.

The polarizability anisotropy (δ) of the groups shown in Figure 1 was calculated using the B3LYP/LanL2DZ method with the Gaussian 09 software. The polarizability anisotropy was calculated according to the following formula (α_{xx}, α_{yy}, α_{zz}, α_{xy}, α_{xz}, α_{yz}; the six independent components of the polarizability tensor):

$$\delta = \Delta\alpha = \sqrt{\frac{(\alpha_{xx} - \alpha_{yy})^2 + (\alpha_{yy} - \alpha_{zz})^2 + (\alpha_{xx} - \alpha_{zz})^2 + 6(\alpha_{xy}^2 + \alpha_{xz}^2 + \alpha_{yz}^2)}{2}}$$

Table S1. Summary of crystallographic data and structure refinements for **LSSC** and **LSSB**.

Formula	**$La_2SbS_3(S_2)Br$**	**$La_2SbS_3(S_2)Cl$**
Formula weight	639.78	595.32
Temperature [K]	100.01(10)	100.00(10)
Crystal system	Orthorhombic	
Space group (number)	*Pnma* (62)	
a [Å]	8.8999(2)	8.7695(2)
b [Å]	5.50600(10)	5.47700(10)
c [Å]	17.8051(4)	17.6929(4)
Volume [Å^3]	872.50(3)	849.80(3)
Z	4	
ρ_{calc} [gcm^{-3}]	4.871	4.653
μ [mm^{-1}]	18.375	14.478
F(000)	1120	1048
Radiation	MoK_α (λ=0.71073 Å)	
R_{int}	0.0473	0.0418
Goodness-of-fit on F^2	1.210	1.048
R_1, wR_2 [$I \geq 2\sigma(I)$][a]	0.0259, 0.0585	0.0191, 0.0418
R_1, wR_2 [all data]	0.0262, 0.0586	0.0199, 0.0422

[a] $R_1 = \Sigma||F_o|-|F_c||/\Sigma|F_o|$ and $wR_2 = \{\Sigma[w(F_o^2-F_c^2)^2]/\Sigma[w(F_o^2)^2]\}^{1/2}$.

Table S2. Atomic coordinates ($\times 10^4$) and equivalent isotropic displacement parameters ($Å^2 \times 10^3$) for **LSSC** and **LSSB**. U_{eq} is defined as 1/3 of the trace of the orthogonalised U_{ij} tensor.

Compounds	Atom	*x*	*y*	*z*	U(eq)
$La_2SbS_3(S_2)Cl$	La1	7654.8(4)	12500	4709.2(2)	7.89(12)
	La2	3443.3(4)	12500	3031.8(2)	6.74(12)
	Sb1	64.7(6)	7500	3333.3(3)	24.60(17)
	Cl1	4128.3(18)	12500	4686.9(9)	9.6(3)
	S1	6541.5(13)	10531(2)	3254.9(7)	12.3(3)
	S2	163.0(19)	2500	3468.9(9)	9.3(3)
	S3	2804.2(18)	7500	3596.9(9)	7.2(3)
	S4	-803.0(19)	7500	4608.7(9)	7.9(3)
$La_2SbS_3(S_2)Br$	La1	1549.6(6)	12500	3003.5(3)	7.58(16)
	La2	2735.3(6)	7500	5290.6(3)	8.49(16)
	Sb1	4868.9(8)	7500	3310.3(4)	23.0(2)
	Br1	957.1(10)	12500	4723.2(5)	8.7(2)
	S1	1548.4(17)	9422(3)	6732.1(9)	9.6(3)
	S2	4802(3)	2500	3466.5(13)	11.3(5)
	S3	2182(2)	7500	3577.1(12)	6.6(4)
	S4	5745(3)	7500	4572.7(13)	8.9(4)

Table S3. Selected bond distances (Å) and bond angles for **LSSC** and **LSSB**.

$La_2SbS_3(S_2)Cl$			
Atom–Atom	Length [Å]	Atom–Atom	Length [Å]
La1–Cl1$^{\#1}$	3.3296(9)	La2–S1$^{\#7}$	3.0211(12)
La1–Cl1$^{\#2}$	3.3296(9)	La2–S1	2.9497(12)
La1–Cl1	3.0928(16)	La2–S1$^{\#3}$	2.9497(12)
La1–S1	2.9558(13)	La2–S2$^{\#8}$	3.0536(17)
La1–S1$^{\#3}$	2.9557(12)	La2–S2$^{\#9}$	2.9787(17)
La1–S2$^{\#4}$	3.1071(17)	La2–S3$^{\#9}$	2.9687(6)
La1–S3$^{\#1}$	3.0239(17)	La2–S3	2.9687(6)
La1–S4$^{\#5}$	3.0594(7)	Sb1–S2$^{\#9}$	2.75034(17)
La1–S4$^{\#1}$	3.0131(17)	Sb1–S2	2.75034(17)
La1–S4$^{\#4}$	3.0594(8)	Sb1–S3	2.4472(17)
La2–Cl1	2.9893(16)	Sb1–S4	2.3814(17)
La2–S1$^{\#6}$	3.0211(12)	S1–S1$^{\#3}$	2.156(3)
Atom–Atom–Atom		Angle [°]	
S2$^{\#9}$–Sb1–S2		169.36(7)	

S3–Sb1–S2		87.28(4)	
S3–Sb1–S2$^{\#9}$		87.28(4)	
S4–Sb1–S2		85.84(4)	
S4–Sb1–S2$^{\#9}$		85.84(4)	
S4–Sb1–S3		97.65(6)	
$La_2SbS_3(S_2)Br$			
Atom–Atom	Length [Å]	Atom–Atom	Length [Å]
La1–Br1	3.1069(10)	La2–S1$^{\#8}$	2.9704(16)
La1–S1$^{\#1}$	3.0184(16)	La2–S1	2.9704(16)
La1–S1$^{\#2}$	2.9907(16)	La2–S2$^{\#9}$	3.115(2)
La1–S1$^{\#3}$	2.9907(16)	La2–S3	3.091(2)
La1–S1$^{\#4}$	3.0184(16)	La2–S4$^{\#10}$	3.0771(11)
La1–S2$^{\#5}$	3.009(2)	La2–S4$^{\#9}$	3.0771(11)
La1–S2$^{\#6}$	3.045(2)	La2–S4	2.968(2)
La1–S3$^{\#5}$	2.9897(9)	Sb1–S2	2.7677(3)
La1–S3	2.9897(9)	Sb1–S2$^{\#5}$	2.7677(3)
La2–Br1	3.3323(6)	Sb1–S3	2.438(2)
La2–Br1$^{\#2}$	3.2863(11)	Sb1–S4	2.379(2)
La2–Br1$^{\#7}$	3.3323(6)	S1–S1$^{\#8}$	2.117(4)
Atom–Atom–Atom		Angle [°]	
S2$^{\#5}$–Sb1–S2		168.20(10)	
S3–Sb1–S2		87.66(5)	
S3–Sb1–S2$^{\#5}$		87.66(5)	
S4–Sb1–S2		84.96(5)	
S4–Sb1–S2$^{\#5}$		84.96(5)	
S4–Sb1–S3		97.89(8)	

Symmetry transformations used to generate equivalent atoms :

LSSC : #1: 1-X, 2-Y, 1-Z; #2: 1-X, 3-Y, 1-Z; #3: 1+X, 1+Y, +Z; #4: +X, 2.5-Y, +Z; #5: 1+X, +Y, +Z; #6: -0.5+X, +Y, 0.5-Z; #7: -0.5+X, 2.5-Y, 0.5-Z; #8: 0.5+X, 1+Y, 0.5-Z; #9: +X, 1+Y, +Z;

LSSB : #1: -X, 2-Y, 1-Z; #2: 0.5-X, 2-Y, -0.5+Z; #3: -X, 0.5+Y, 1-Z; #4: 0.5-X, 0.5+Y, -0.5+Z; #5: +X, 1+Y, +Z; #6: -0.5+X, 1+Y, 0.5-Z; #7: +X, -1+Y, +Z; #8: +X, 1.5-Y, +Z; #9: 1-X, 1-Y, 1-Z; #10: 1-X, 2-Y, 1-Z.

Table S4. Comprehensive statistics of Δn and E_g between **LSSC**, **LSSB**, and some typical

chalcogenide birefringent crystals with Δn > 0.1 and E_g > 1.0 eV.

	Compound	Δn(@546 nm)	E_g (eV)	Reference
1	Ag_3AsS_3(*R*3*c*)	0.237	2.03	[7]
2	$AsPS_4$	0.268	2.70	[8]
3	$Ba_{13}(BS_3)_6(SnS_6)$	0.264	2.69	[9]
4	Ba_2AlSbS_5	0.241	2.57	[10]
5	$Ba_2As_2S_5$	0.187	2.02	[11]
6	Ba_2AsS_3Br	0.178	2.8	[12]
7	Ba_2AsS_3Cl	0.187	2.8	[12]
8	Ba_2AsS_3I	0.180	2.8	[12]
9	Ba_2SbS_3I	0.195	2.64	[12]
10	$Ba_3(BS_3)(PS_4)$	0.124	3.4	[13]
11	$Ba_6(BS_3)_3(BiS_3)$	0.159	2.43	[14]
12	$Ba_6(BS_3)_3(SbS_3)$	0.157	3.01	[14]
13	$BaAgSbS_3$	0.263	2.2	[15]
14	$BaBi(BS_3)S$	0.696	2.34	[16]
15	$BaCd_2As_2S_6$	0.169	2.60	[17]
16	BaFS	0.238	2.75	[18]
17	$BaSbBS_4$	0.943	2.70	[19]
18	$BaSnS_2$	0.381	2.4	[20]
19	$BaTeSeS_2$	0.55	1.82	[21]
20	$Cs_2Ag_2As_2S_5$	0.247	2.48	[22]
21	$Cs_2Ag_3Sb_3S_7$	0.352	2.02	[23]
22	$Cs_2Ba_3Cu_2Sb_2S_{10}$	0.441	1.98	[24]
23	$Cs_2Cu_2Sb_2S_5$	0.490	1.6	[25]
24	$Cs_2HgSb_4S_8$	0.185	2.13	[26]
25	$Cs_2Sb_2Sn_3S_{10}$	0.140	2.34	[27]
26	$Cs_2ZnSb_2S_5$	0.417	2.16	[28]

27	**$Cs_2ZnSn_3S_8$**	**0.12**	**3.20**	[29]
28	**$Cs_3CuAs_4S_8$**	**0.184**	**2.26**	[30]
29	**$Cs_4Sb_4S_8$**	**0.433**	**2.11**	[31]
30	**$CsAg_2AsS_3$**	**0.200**	**2.70**	[32]
31	**$CsAg_2SbS_3$**	**0.337**	**2.05**	[33]
32	**$CsAgSb_4S_7$**	**0.689**	**2.04**	[34]
33	**$CsCu_2AsS_3$**	**0.493**	**2.26**	[35]
34	**$CsHgAsS_3$**	**0.220**	**2.64**	[36]
35	**$CsSb_5S_8$**	**0.789**	**1.87**	[37]
36	**$CsZnAsSe_3$**	**0.223***	**2.25**	[38]
37	**$CuSbS_2$**	**0.503**	**1.52**	[39]
38	**$Hg_4InS_2Cl_5$**	**0.351**	**3.1**	[40]
39	**$InSb_2S_4Br$**	**1.253**	**1.80**	[41]
40	**$InSb_2S_4Cl$**	**1.340**	**1.80**	[41]
41	**$K_2Ba_3Cu_2Sb_2S_{10}$**	**0.453**	**1.90**	[24]
42	**$K_2Sb_2Sn_3S_{10}$**	**0.161**	**2.30**	[27]
43	**KAg_2AsS_3**	**0.336**	**2.25**	[42]
44	**KAg_2SbS_3**	**0.335**	**2.1**	[43]
45	**KCu_2SbS_3**	**0.428**	**1.7**	[44]
46	**$KGa_2In_3S_8$**	**0.134**	**2.85**	[45]
47	**KSb_5S_8**	**0.385**	**1.61**	[37]
48	**La_2CuSbS_5**	**0.265**	**2.06**	[46]
49	**$LaBS_3$**	**0.169**	**3.18**	[47]
50	**$LaSbS_2Br_2$**	**0.102**	**2.72**	[48]
51	**$LiAsS_2$**	**0.536**	**1.60**	[49]
52	**$LiSrSbS_3$**	**0.359**	**2.30**	[50]
53	**$NaAsS_2$**	**0.628**	**2.23**	[49]
54	**$NaBaSbS_3$**	**0.30**	**2.46**	[51]
55	**$NaBaSbSe_3$**	**0.38**	**1.74**	[51]

56	**$NaGaS_2$**	**0.133**	**3.92**	[52]
57	**α-$NaSbP_2S_6$**	**0.232**	**2.17**	[53]
58	**β-$NaSbP_2S_6$**	**0.129**	**2.25**	[53]
59	**β-$Pb_3P_2S_8$**	**0.23**	**2.37**	[54]
60	**$PbSbBS_4$**	**1.059**	**1.75**	[55]
61	**$Rb_2Ag_3Sb_3S_7$**	**0.354**	**2.11**	[23]
62	**$Rb_2Ba_3Cu_2Sb_2S_{10}$**	**0.450**	**1.93**	[24]
63	**$Rb_2Cu_2Sb_2S_5$**	**0.425**	**1.6**	[25]
64	**$Rb_2HgSb_4S_8$**	**0.211**	**1.82**	[56]
65	**$Rb_2Sb_2Sn_3S_{10}$**	**0.146**	**2.33**	[27]
66	**$Rb_2ZnSb_4S_8$**	**0.243**	**1.88**	[57]
67	**$Rb_3NaSn_3Se_8$**	**0.227**	**1.71**	[58]
68	**$Rb_8Cu_6As_8S_{19}$**	**0.101**	**1.8**	[25]
69	**$RbAg_2AsS_3$**	**0.323**	**2.30**	[33]
70	**$RbCu_2AsS_3$**	**0.277**	**1.96**	[59]
71	**$RbSb_5S_8$**	**0.387**	**1.60**	[37]
72	**$[RbSr_3Br][(BS_3)_2]$**	**0.166**	**3.70**	[60]
73	**$[RbSr_3Cl][(BS_3)_2]$**	**0.155**	**3.64**	[60]
74	**$Sn_2Ga_2S_5$**	**0.172**	**2.02**	[61]
75	**Sn_2SiS_4**	**0.192**	**2.00**	[62]
76	**LSSB**	**1.057**	**2.29**	**This work**
77	**LSSC**	**1.049**	**2.22**	**This work**

*: experimental value; The theoretical birefringence of some compounds was calculated by us based on the experimental band gaps and crystal structures provided in the original literature.

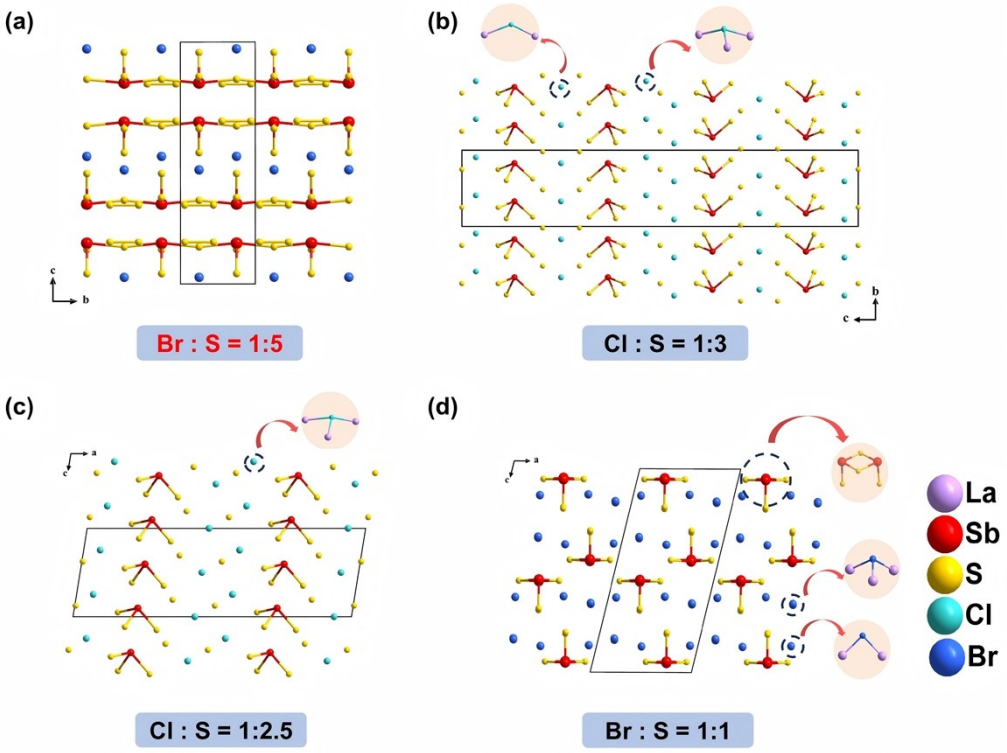

Figure S1. Comparison of Cl/Br:S molar ratios and the assembly modes of the anionic groups in (a) **LSSB**, (b) $La_5Sb_2S_9Cl_3$, (c) $La_3SbS_5Cl_2$ and (d) $LaSbS_2Br_2$. The birefringence values for the compounds in Figures a–d are 1.057, 0.052, 0.084, 0.102 at 546 nm, respectively.

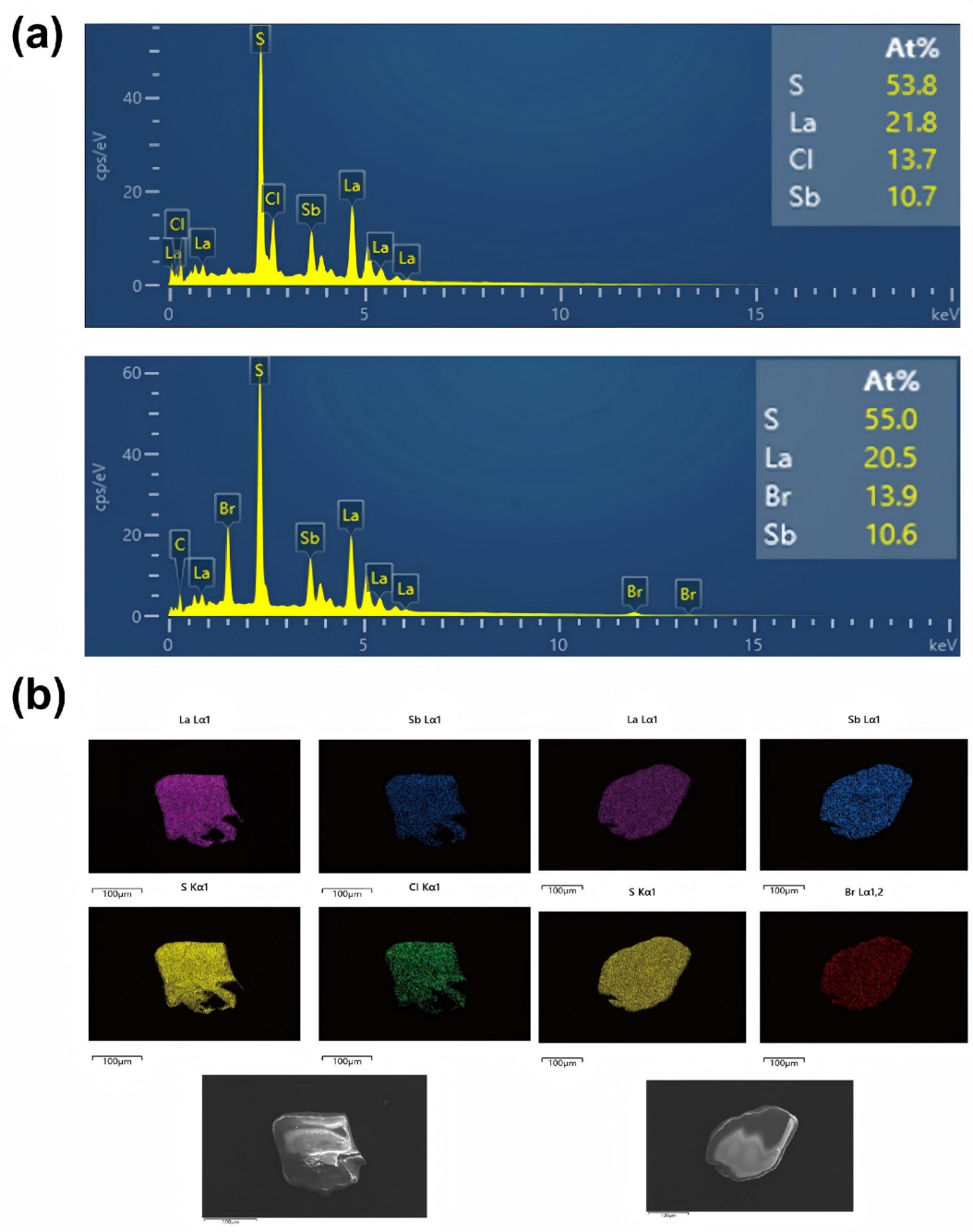

Figure S2. Elemental analyses of **LSSC** and **LSSB**: (a) energy-dispersive X-ray spectroscopy; (b) SEM images and corresponding elemental distribution mapping analyses.

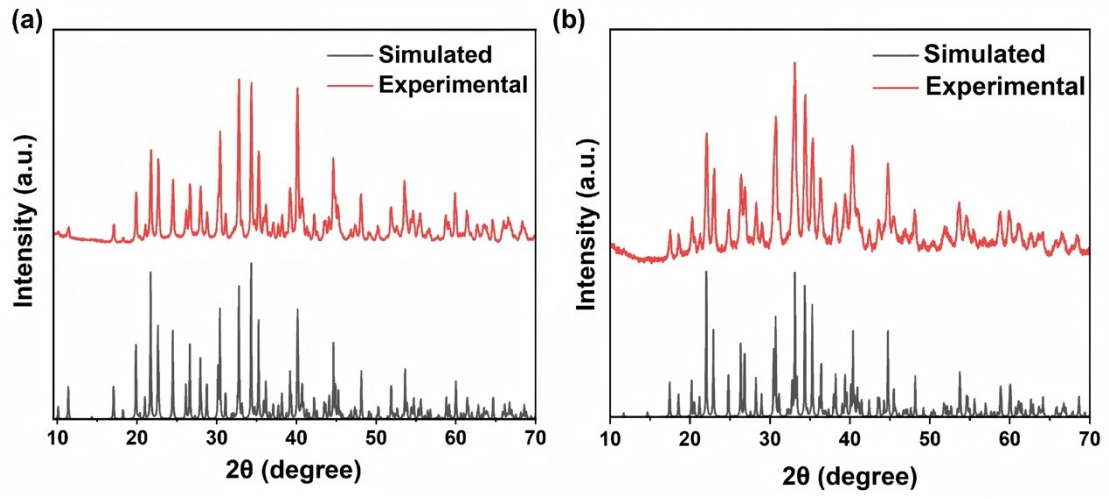

Figure S3. Simulated and experimental powder X-ray diffractometer patterns of (a) **LSSC** and (b) **LSSB**.

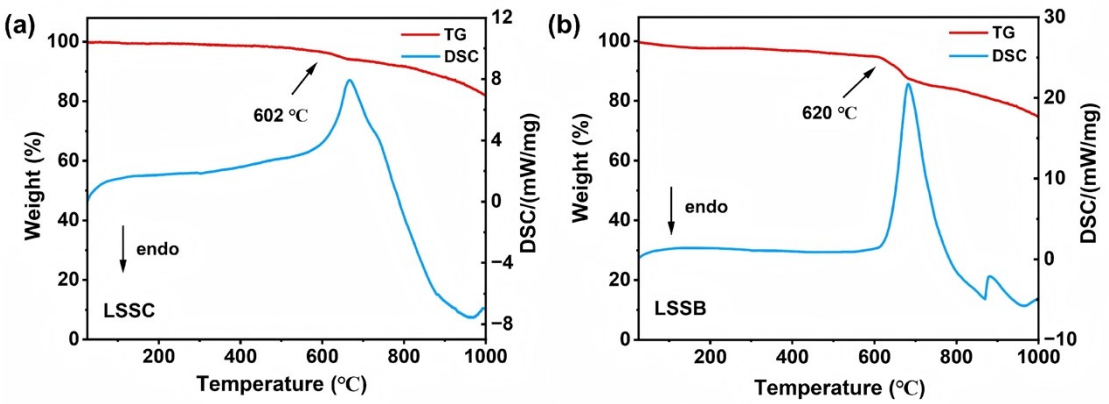

Figure S4. The TG-DSC curves of (a) **LSSC** and (b) **LSSB**.

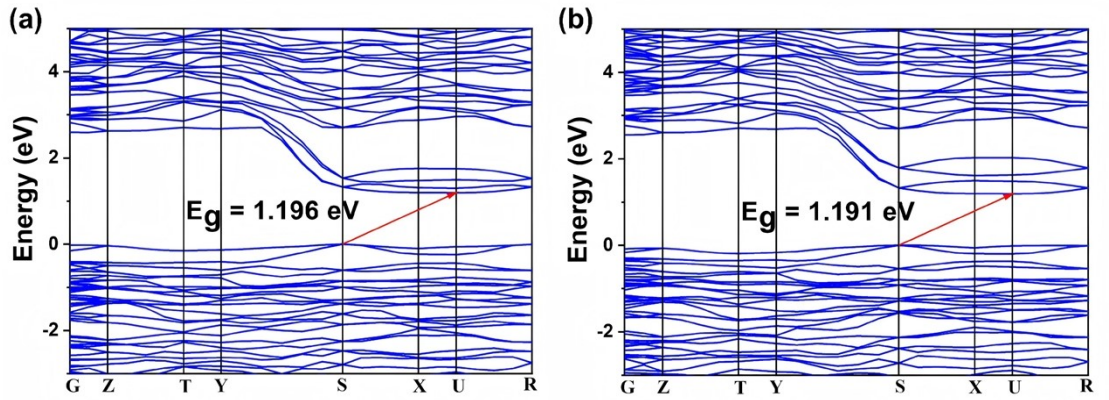

Figure S5. The band structures of (a) **LSSC** and (b) **LSSB**.

References

1 G. M. Sheldrick, SHELXT-Integrated Space-Group and Crystal-Structure Determination, *Acta Crystallogr., Sect. A: Found. Adv.*, 2015, **71**, 3–8.

2 A. L. Spek, Single-Crystal Structure Validation with the Program PLATON, *J. Appl. Crystallogr.*, 2003, **36**, 7–13.

3 V. Milman, B. Winkler, J. A. White, C. J. Pickard, M. C. Payne, E. V. Akhmatskaya and R. H. Nobes, Electronic Structure, Properties, and Phase Stability of Inorganic Crystals: A Pseudopotential Plane-Wave Study, *Int. J. Quantum Chem.*, 2000, **77**, 895–910.

4 M. D. Segall, P. J. D. Lindan, M. J. Probert, C. J. Pickard, P. J. Hasnip, S. J. Clark and M. C. Payne, First-Principles Simulation: Ideas, Illustrations and the CASTEP Code, *J. Phys.: Condens. Matter*, 2002, **14**, 2717–2744.

5 J. P. Perdew, K. Burke and M. Ernzerhof, Generalized Gradient Approximation Made Simple, *Phys. Rev. Lett.*, 1997, **77**, 3865–3868.

6 J. S. Lin, A. Qteish, M. C. Payne and V. Heine, Optimized and Transferable Nonlocal Separable Ab Initio Pseudopotentials, *Phys. Rev. B*, 1993, **47**, 4174–4180.

7 R. Zhao, J. Zhou, X. Liu, R. Li and Q. Tang, A New Solvothermal Route to Crystalline Proustite Ag_3AsS_3 with Photocatalytic Properties, *Inorg. Chem. Commun.*, 2014, **46**, 17–20.

8 C. D. Morris, E. K. Qian, P. E. Meza, V. K. Sangwan, C. D. Malliakas, M. C. Hersam and M. G. Kanatzidis, Nanotube Structure of $AsPS_{4-x}Se_x$ (x = 0, 1), *Inorg. Chem.*, 2024, **63**, 4915–4924.

9 M. A. Khan, J.-Q. Wang, P.-F. Liu, L. Chen and Y.-Y. Li, $Ba_{13}(BS_3)_6(SnS_6)$: Synthesis, Crystal Structure, Electronic Structure, and Optical Propertyæ, *Chinese J. Struct. Chem.*, 2017, **36**, 204–210.

10 X. Wu, X. Gu, H. Pan, Y. Hu and K. Wu, Synthesis, Crystal Structures, Optical Properties and Theoretical Calculations of Two Metal Chalcogenides Ba_2AlSbS_5 and $Ba_2GaBiSe_5$, *Crystals*, 2018, **8**, 165.

11 A. K. Iyer, J. B. Cho, M. J. Waters, J. S. Cho, B. M. Oxley, J. M. Rondinelli, J. I. Jang and M. G. Kanatzidis, Ba_2MAsQ_5 (Q = S and Se) Family of Polar Structures with Large Second Harmonic Generation and Phase Matchability, *Chem. Mater.*, 2022, **34**, 5283–5293.

12 R. Wang, X. Zhang, J. He, K. Bu, C. Zheng, J. Lin and F. Huang, Synthesis, Structure, and Optical Properties of Antiperovskite-Derived Ba_2MQ_3X (M = As, Sb; Q = S, Se; X = Cl, Br, I) Chalcohalides, *Inorg. Chem.*, 2018, **57**, 1449–1454.

13 J. Zhou, L. Wang, H. Wang, L. Luo, J. Li and F. Yu, $Ba_3(BS_3)(PS_4)$: The First Alkaline-Earth Metal Thioborate–Thiophosphate with Strong Optical Anisotropy Originating from Planar [BS_3] Units, *Dalton Trans.*, 2023, **52**, 16113–16117.

14 Y.-Y. Li, B.-X. Li, G. Zhang, L.-J. Zhou, H. Lin, J.-N. Shen, C.-Y. Zhang, L. Chen and L.-M. Wu, Syntheses, Characterization, and Optical Properties of Centrosymmetric $Ba_3(BS_3)_{1.5}(MS_3)_{0.5}$ and Noncentrosymmetric $Ba_3(BQ_3)(SbQ_3)$, *Inorg. Chem.*, 2015, **54**, 4761–4767.

15 C. Liu, Y. Shen, P. Hou, M. Zhi, C. Zhou, W. Chai, J.-W. Cheng and Y. Liu, Hydrazine-Hydrothermal Synthesis and Characterization of the Two New Quaternary Thioantimonates(III) $BaAgSbS_3$ and $BaAgSbS_3 \cdot H_2O$, *Inorg. Chem.*, 2015, **54**, 8931–8936.

16 L. Geng, W.-D. Cheng, W.-L. Zhang, C.-S. Lin, H. Zhang, Y.-Y. Li and Z.-Z. He, $BaM(BS_3)S$ (M = Sb, Bi): Two New Thioborate Compounds with One-Dimensional Polymeric Chain Structure, *Inorg. Chem.*, 2010, **49**, 6609–6615.

17 Y. Guo, F. Liang, M. Zhou, Z. Lin, J. Yao and Y. Wu, $BaM_2As_2S_6$ (M = Cd, Hg): Synthesis, Crystal Structure, Optical and Electronic Properties, *J. Alloys Compd.*, 2018, **762**, 143–148.

18 C. Xie, X. Jiang, B. Liu and G. Guo, BaFS: Birefringence Enhanced by the Transformation from Optical Isotropy to Anisotropy via Interlayer Anion Substitution, *Small*, 2025, **21**, 2409705.

19 M.-Z. Zhang, Y. Zhao, C.-L. Hu and J.-G. Mao, $BaSbBS_4$: A Record-High-Performance Birefringent Crystal Identified by a Target-Driven Closed-Loop Strategy, *Chem. Sci.*, 2025, **16**, 12577–12586.

20 W. D. C. B. Gunatilleke, A. F. May, A. R. H. Walker, A. J. Biacchi and G. S. Nolas, Synthesis, Crystal Structure, and Physical Properties of $BaSnS_2$, *Phys. Status Solidi (RRL)–Rapid Res. Lett.*, 2022, **16**, 2100624.

21 B. Zhang, W. Huang, J. Zhang, X. Wu, H. Lin and Q. Zhu, $[TeSeS_2]^{2-}$: The First Heterotriple-Chalcogenide Motifs Decode Giant Mid-Far Infrared Birefringence, *Angew. Chem. Int. Ed.*, 2025, **64**, e202508555.

22 D. Yan, Y. Xiao, C. Liu, P. Hou, W. Chai, H. Hosono, H. Lin and Y. Liu, Two New Members in the Quaternary Cs–Ag–As–S Family with Different Arrangements of Ag-S and As-S Asymmetric Building Units: Syntheses, Structures, and Theoretical Studies, *Dalton Trans.*, 2020, **49**, 9743–9750.

23 G. Yang, L.-H. Li, C. Wu, M. G. Humphrey and C. Zhang, Ionothermal Synthesis of Metal Chalcogenides $M_2Ag_3Sb_3S_7$ (M = Rb, Cs) Displaying Nonlinear Optical Activity in the Infrared Region, *Inorg. Chem.*, 2019, **58**, 12582–12589.

24 C. Liu, Y. Xiao, H. Wang, W. Chai, X. Liu, D. Yan, H. Lin and Y. Liu, One-Dimensional Chains in Pentanary Chalcogenides $A_2Ba_3Cu_2Sb_2S_{10}$ (A = K, Rb, Cs) Displaying a Photocurrent Response, *Inorg. Chem.*, 2020, **59**, 1577–1581.

25 C. Zhang, M. Ji, S.-H. Ji and Y.-L. An, Mild Solvothermal Syntheses and Characterization of Layered Copper Thioantimonates(III) and Thioarsenate(III), *Inorg. Chem.*, 2014, **53**, 4856–4860.

26 C.-X. Du, F.-Y. Qi, J. Chen and M. Baiyin, Two Mercury Antimony Chalcogenides $Cs_2HgSb_4S_8$ and $Cs_2Hg_2Sb_2Se_6$ with Cesium Cations as Counterions, *ACS Omega*, 2018, **3**, 15168–15173.

27 J. P. Yohannan and K. Vidyasagar, Syntheses and Characterization of One-Dimensional Alkali Metal Antimony(III) Thiostannates(IV), $A_2Sb_2Sn_3S_{10}$ (A=K, Rb, Cs), *J. Solid State Chem.*, 2015, **221**, 426–432.

28 N. Li, G. Teri, M. Shele, Sagala, Namila and M. Baiyin, The Solvothermal Synthesis and Properties of Thioantimonates Rb(1,4-DABH)Sb_4S_7 and $Cs_2ZnSb_2S_5$: 1D Anion

Chains and 2D Anion Layer, *J. Cluster Sci.*, 2023, **34**, 1853–1860.

29 T. Tian, Z. Li, N. Wang, S. Zhao, J. Xu, Z. Lin and D. Mei, $Cs_2ZnSn_3S_8$: A Sulfide Compound Realizes a Large Birefringence by Modulating the Dimensional Structure, *Inorg. Chem.*, 2021, **60**, 9248–9253.

30 C. Liu, H.-D. Yang, P.-P. Hou, Y. Xiao, Y. Liu and H. Lin, $Cs_3CuAs_4Q_8$ (Q = S, Se): Unique Two-Dimensional Layered Inorganic Thioarsenates with the Lowest Cu-to-As Ratio and Remarkable Photocurrent Responses, *Dalton Trans.*, 2022, **51**, 904–909.

31 F.-Y. Qi, M. Shele and M. Baiyin, Two Ternary Antimony-Chalcogenides of $Cs_4Sb_4S_8$ and $Cs_3Sb_5Se_9$, *Inorg. Chem. Commun.*, 2021, **129**, 108635.

32 H.-G. Yao, P. Zhou, S.-H. Ji, R.-C. Zhang, M. Ji, Y.-L. An and G.-L. Ning, Syntheses and Characterization of a Series of Silver-Thioantimonates(III) and Thioarsenates(III) Containing Two Types of Silver-Sulfur Chains, *Inorg. Chem.*, 2010, **49**, 1186–1190.

33 Y. Li, X. Song, Y. Zhong, Y. Guo, M. Ji, Z. You and Y. An, Temperature Controlling Valance Changes of Crystalline Thioarsenates and Thioantimonates, *J. Alloys Compd.*, 2021, **872**, 159591.

34 F. Q. Huang and J. A. Ibers, Synthesis, Structure, Band Gap, and Electronic Structure of $CsAgSb_4S_7$, *J. Solid State Chem.*, 2005, **178**, 212–217.

35 Y. Li, X. Cao, M. Ji, Z. You and Y. An, Solvothermal Syntheses, Structures, and Characterizations of Four Thioarsenates $A_7Cu_4As_3S_{13}$ (A = Rb, Cs), $Rb_2Cu_5As_3S_8$, and $CsCu_2AsS_3$, *Inorg. Chem. Commun.*, 2022, **139**, 109365.

36 Y. Sun, Y. Li, Y. Guo, Y. Liu, X. Cao, M. Ji, Z. You and Y. An, Solvothermal Syntheses, Crystal Structures, and Photoelectric Response Properties of Two Quaternary Mercury-Thioarsenates(III), *Inorg. Chem. Commun.*, 2021, **123**, 108303.

37 W.-F. Chen, B.-W. Liu, S.-M. Pei, Q.-N. Yan, X.-M. Jiang and G.-C. Guo, ASb_5S_8 (A = K, Rb, and Cs): Thermal Switching of Infrared Nonlinear Optical Properties across the Crystal/Glass Transformation, *Chem. Mater.*, 2021, **33**, 3729–3735.

38 C. Zhang, M.-Y. Ran, X. Chen, S.-H. Zhou, H. Lin and Y. Liu, Stereochemically Active Lone-Pair-Driven Giant Enhancement of Birefringence from Three-Dimensional $CsZn_4Ga_5Se_{12}$ to Two-Dimensional $CsZnAsSe_3$, *Inorg. Chem. Front.*, 2023, **10**, 3367–3374.

39 J. T. R. Dufton, A. Walsh, P. M. Panchmatia, L. M. Peter, D. Colombara and M. S. Islam, Structural and Electronic Properties of $CuSbS_2$ and $CuBiS_2$: Potential Absorber Materials for Thin-Film Solar Cells, *Phys. Chem. Chem. Phys.*, 2012, **14**, 7229.

40 Q. Ren, Y. Chu, W. Jin, M. Chen, C. Cui, Y. Wu and S. Pan, $Hg_4InS_2Cl_5$: Achieving Giant Optical Anisotropy by Introducing Well-Aligned Linear $[Hg_2S_2]$ Units, *Adv. Opt. Mater.*, 2025, **13**, 2402170.

41 L. Wang and S.-J. Hwu, A New Series of Chalcohalide Semiconductors with Composite $CdBr_2/Sb_2Se_3$ Lattices: Synthesis and Characterization of $CdSb_2Se_3Br_2$ and Indium Derivatives $InSb_2S_4X$ (X = Cl and Br) and InM_2Se_4Br (M = Sb and Bi), *Chem. Mater.*, 2007, **19**, 6212–6221.

42 D. Yan, P. Hou, C. Liu, W. Chai, X. Zheng, L. Zhang, M. Zhi, C. Zhou and Y. Liu, Effect of Alkali Cations on Two-Dimensional Networks of Two New Quaternary

Thioarsenates (III) Prepared by a Facile Surfactant-Thermal Method, *J. Solid State Chem.*, 2016, **241**, 47–53.

43 H.-G. Yao, M. Ji, S.-H. Ji, R.-C. Zhang, Y.-L. An and G. Ning, Solvothermal Syntheses of Two Novel Layered Quaternary Silver−Antimony(III) Sulfides with Different Strategies, *Cryst. Growth Des.*, 2009, **9**, 3821–3824.

44 R. Wang, X. Zhang, J. He, C. Zheng, J. Lin and F. Huang, Synthesis, Crystal Structure, Electronic Structure, and Photoelectric Response Properties of KCu_2SbS_3, *Dalton Trans.*, 2016, **45**, 3473–3479.

45 Y. Xie, W.-D. Yao, Q.-Y. Du, W. Zhou, N.-T. Suen, W. Liu and S.-P. Guo, From $NaSc_3Ga_2Q_8$ (Q = S, Se) to $KGa_2In_3S_8$: Substitution of Sc^{3+} with In^{3+} to Achieve Doubled Birefringence, *Chem. Sci.*, 2025, **16**, 17207–17213.

46 H. Lin, Y.-Y. Li, M.-Y. Li, Z. Ma, L.-M. Wu, X.-T. Wu and Q.-L. Zhu, Centric-to-Acentric Structure Transformation Induced by a Stereochemically Active Lone Pair: A New Insight for Design of IR Nonlinear Optical Materials, *J. Mater. Chem. C*, 2019, **7**, 4638–4643.

47 Y.-X. Han, C.-L. Hu, Z. Fang, Q.-Q. Chen, B.-X. Li, Y. Lin and J.-G. Mao, $LaBS_3$ Revisited: A Promising Mid-Infrared Nonlinear Optical Material, *J. Mater. Chem. C*, 2022, **10**, 12556–12559.

48 D. Gout, S. Jobic, M. Evain and R. Brec, New Antimony Lanthanide Disulfide Dibromides $LnSbS_2Br_2$ (Ln = La, Ce): Crystal and Electronic Structures and Optical Properties, *J. Solid State Chem.*, 2001, **158**, 218–226.

49 T. K. Bera, J. Song, A. J. Freeman, J. I. Jang, J. B. Ketterson and M. G. Kanatzidis, Soluble Direct-Band-Gap Semiconductors $LiAsS_2$ and $NaAsS_2$: Large Electronic Structure Effects from Weak As···S Interactions and Strong Nonlinear Optical Response, *Angew. Chem. Int. Ed.*, 2008, **47**, 7828–7832.

50 A. Yalikun, K. Zhang, J. Han and Z. Yang, $LiSrSbS_3$: Parallel Configurations of Lone Pair Electrons Inducing a Large Birefringence, *Dalton Trans.*, 2022, **51**, 14545–14550.

51 A. Abudurusuli, K. Wu, A. Tudi, Z. Yang and S. Pan, $ABaSbQ_3$ (A = Li, Na; Q = S, Se): Diverse Arrangement Modes of Isolated SbQ_3 Ligands Regulating the Magnitudes of Birefringences, *Chem. Commun.*, 2019, **55**, 5143–5146.

52 Y. Yun, W. Xie, Z. Yang, G. Li and S. Pan, Na^+/Ag^+ Substitution Induced Birefringence Enhancement from $AgGaS_2$ to $NaGaS_2$, *J. Alloys Compd.*, 2022, **896**, 163093.

53 V. Manríquez, A. Galdámez and D. Ruiz-León, Preparation, Crystal Structure and Characterization of α-$NaSbP_2S_6$ and β-$NaSbP_2S_6$ Phases, *Mater. Res. Bull.*, 2006, **41**, 1337–1344.

54 W. Guo, Y. Zhu, H.-H. Cui, L. Li, Y. Yu, Z.-Z. Luo and Z. Zou, β-$Pb_3P_2S_8$: A New Optical Crystal with Exceptional Birefringence Effect, *Chin. Chem. Lett.*, 2025, **36**, 110256.

55 L. Geng, W.-D. Cheng, W.-L. Zhang, Y.-Y. Li, Z.-Z. Luo, H. Zhang, C.-S. Lin and Z.-Z. He, Syntheses, Crystal Structures and Characterizations of Two New Quaternary Thioborates: $PbMBS_4$ (M = Sb, Bi), *Dalton Trans.*, 2011, **40**, 4474.

56 G. Yang, C. Wu, J. Zhang and C. Zhang, Multinary Thioantimonates(III) with d^{10} Transition Metals: Ionothermal Synthesis, Crystal Structures and Physical Properties, *J. Cluster Sci.*, 2022, **33**, 1569–1577.

57 M. Shele, X. Tian and M. Baiyin, Solvothermal Synthesis and Properties of Three Antimony Chalcogenides Containing Transition Metal Zinc, *J. Solid State Chem.*, 2021, **302**, 122401.

58 X. Ji, H. Wu, B. Zhang, H. Yu, Z. Hu, J. Wang and Y. Wu, Intriguing Dimensional Transition Inducing Variable Birefringence in $K_2Na_2Sn_3S_8$ and $Rb_3NaSn_3Se_8$, *Inorg. Chem.*, 2021, **60**, 1055–1061.

59 H.-G. Yao, C.-F. Tang, Y.-L. An, Z.-J. Ou, G.-H. Wu, P. Lan and Y.-L. Zheng, Solvothermal Syntheses and Characterization of Three New Silver(I)/Copper(I)-Thioarsenates Based on As^{2+}/As^{3+} Ions, *J. Solid State Chem.*, 2017, **246**, 87–91.

60 Y. Yun, X. Hou, Z. Yang, G. Li and S. Pan, $[RbSr_3X][(BS_3)_2]$ (X = Cl, Br): Two Salt-Inclusion Thioborates with Large Birefringence and Structure Transformation from Centrosymmetric to Asymmetric, *Chem. Commun.*, 2024, **60**, 118–121.

61 Z.-H. Shi, Y. Chi, Z.-D. Sun, W. Liu and S.-P. Guo, $Sn_2Ga_2S_5$: A Type of IR Nonlinear-Optical Material, *Inorg. Chem.*, 2019, **58**, 12002–12006.

62 C. Li, Z. Lin, L. Kang, Z. Lin, H. Huang, J. Yao and Y. Wu, Sn_2SiS_4, synthesis, structure, optical and electronic properties, *Opt. Mater.*, 2015, **47**, 379–385.